Reaction of a Bulky β-Diketiminato Magnesium Hydride with CO 2 Yielding a Polynuclear Magnesium Cage Compound

Wimonsiri Huadsai, Laure Vendier, Matthias Westerhausen, Sébastien Bontemps

Journal of Inorganic and General Chemistry
ZAAC
Zeitschrift für anorganische und allgemeine Chemie
www.zaac.wiley-vch.de
RESEARCH ARTICLE
DOI: 10.1002/zaac.202400070

Reaction of a Bulky β-Diketiminato Magnesium Hydride with CO_2 Yielding a Polynuclear Magnesium Cage Compound

Wimonsiri Huadsai,[a, b] Laure Vendier,[a] Matthias Westerhausen,*[b] and Sébastien Bontemps*[a]

Dedicated to Prof. Dr. Dr. h.c. Michael Veith on the occasion of his 80th birthday.

The reaction of a sterically shielded Mg hydride complex, bearing a bulky β-diketiminato (BDI) ligand, with CO_2 leads to the formation of polynuclear complexes. CO_2 not only inserts into the metal hydride bond yielding formate ions, but also adds onto the γ-C of the BDI ligand. This reactivity gives rise to the formation of soluble tri- and tetranuclear structures in THF, leading to a hexameric structure associated with a change in the coordination mode of the BDI ligand at 60 °C in THF within four days. The insoluble hexameric complex was isolated in high reproducible yield from the solution and characterized by X-ray diffraction analysis. The reaction affording the hexameric complex was shown to be completed within 1 h at room temperature in toluene. Similar reactions of CO_2 with a BDI calcium hydride complex proceeds less cleanly and a pure product could not be isolated.

Introduction

Ligands with a β-diketiminate (BDI) or nacnac core have been used to stabilize and modify the properties of a large variety of metal centers.[1–2] One of the remarkable properties of this ligand platform is its ligand-based reactivity, notably through the nucleophilic carbon atom in gamma position (γ-C) of its backbone. In 1998, an initial report by Jordan *et al.* indeed showed the cycloaddition of ethylene onto the Al complex **A** featuring a β-diketiminato ligand.[3] The reaction occurred with a bifunctional activation of the C=C bond across the nucleophilic γ-C and the cationic Al centers to give complex **B** (Scheme 1a). Following this initial example, several apolar and polar substrates have then been shown to react in a similar manner.[2]

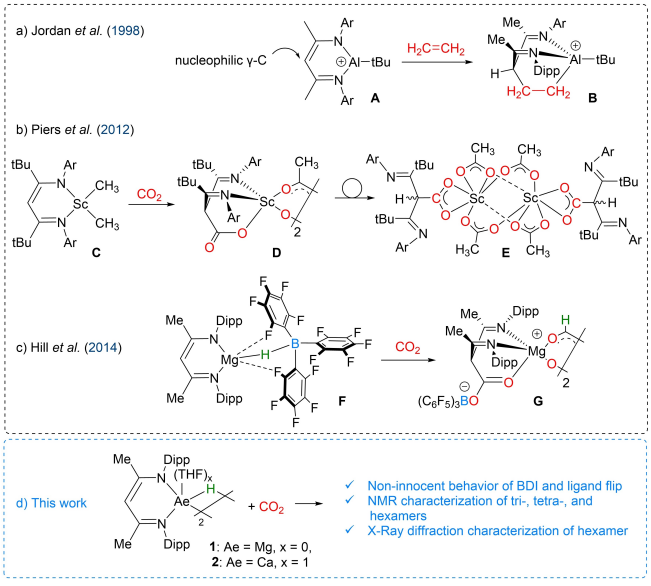

Scheme 1. Bifunctional reactivity with complexes bearing β-diketiminate ligands: a) initial demonstration of reactivity of the γ-C in complex A, b) and c) reactivity of β-diketiminate Mg and Sc complexes C and F toward CO_2, d) general scheme representing the reactivity of complexes 1 and 2 toward CO_2 presented herein.

Among these substrates, the electrophilic carbon atom of CO_2 was shown to react with the γ-C of BDI ligands in the case of Mg and Sc complexes (Scheme 1b and 1c). In 2012, Piers *et al.* showed addition of CO_2 onto the γ-C and insertion into the Sc–Me functionality of the (BDI)Sc$(CH_3)_2$ complex **C** leading to the dimer **D** with bridging acetate ions (Scheme 1b).[4] The detailed study demonstrated that this dimer **D** appeared as a mixture of isomers and was in equilibrium with the monomeric

[a] Dr. W. Huadsai, Dr. L. Vendier, Dr. S. Bontemps
LCC–CNRS
Université de Toulouse, CNRS
1205 route de Narbonne, 31077 Toulouse Cedex 04, France
E-mail: sebastien.bontemps@lcc-toulouse.fr
[b] Dr. W. Huadsai, Prof. M. Westerhausen
Institute of Inorganic and Analytical Chemistry
Friedrich Schiller University Jena (FSU)
Humboldtstraße 8, D-07743 Jena, Germany
E-mail: m.we@uni-jena.de

Supporting information for this article is available on the WWW under https://doi.org/10.1002/zaac.202400070

form depending on the steric hindrance of the ligand caused by the *N*-bound aryl groups and the experimental conditions. The CO_2 addition eventually led to a coordination flip of the BDI ligand via decoordination of the two imine bases and coordination of the newly formed carboxylate moiety affording complex **E** (Scheme 1b). Such flip of the BDI ligand has rarely been reported, presumably because of stability issues with such coordination. It was nonetheless reported in the reactions between i) a Ni complex and CS_2[5] and ii) Sn or Pb compounds and phenylisocyanate.[6] In the latter cases, the flip of the BDI ligand occurred along a proton shift between the γ-CH moiety and one imine of the BDI. In 2014, Hill *et al.* demonstrated that the adduct **F** between $B(C_6F_5)_3$ and a (BDI)Mg(H) complex experiences insertion of CO_2 into the Mg–H bond and attack at the γ-C of the BDI ligand leading to the formation of the dimeric complex **G** (Scheme 1c).[7] Reactivity at the Mg center and at the γ-C atom of the BDI unit was observed for the reaction of (BDI)Mg(tmp) (tmp = 2,2,6,6-tetramethylpiperidide) with the comparable heterocumulene system of isocyanates.[8] This reactivity of the γ-C position had also been found for the reaction of the lithium congener (tmeda)Li(BDI) with CO_2 with the newly formed carboxylate binding to the lithium ion.[9] Again, isocyanates, isothiocyanates, and carbodiimides reacted similarly with the Li(BDI) complex.[10]

The interest for alkaline earth (Ae) metal complexes, especially of non-toxic magnesium and calcium, is linked to their global abundance and the desire to understand their specific reactivity. In this field, Ae complexes featuring a hydride ligand such as complexes **1**[11] and **2**[12] have been key to evaluate elementary steps.[13–17] In CO_2 chemistry, Ae based complexes have been involved in catalytic hydrosilylation[18,19] and hydroboration.[7,20–23] Combining our interest in CO_2 hydroboration[24–29] and Ae chemistry,[30–34] we recently reported that the β-diketiminato Mg and Ca hydride complexes **1** and **2** are efficient catalysts for the selective 4e-reduction of CO_2 using 9-BBN and $HBCy_2$ (dicyclohexylborane) as reductants.[23] We subsequently showed that the obtained bis(boryl)acetal compounds gave rise to original reactivity toward thiol substrates. Complementary to catalytic transformations, stoichiometric studies are important to propose elementary steps as shown by Hill *et al.* with complex **F**[4] and others.[19,35]

With this in mind, we set to study the stoichiometric reactivity of CO_2 with the magnesium and calcium hydride complexes **1**[11] and **2**[12] featuring the β-diketiminato ligand (Scheme 1d). Herein, we report the rich and dynamic chemistry of this dinuclear β-diketiminato Mg hydride complex toward CO_2 and show that it readily reacts with CO_2 both at the hydride moiety and at the γ-C atom of the ligand backbone to afford polynuclear species. In contrast, the related chemistry of the calcium congener proceeds less cleanly.

Results and Discussion

Generation and characterization of Mixture 3. When exposed to 1 atm of $^{13}CO_2$ in THF-d_8, complex **1** fully reacted within 10 min as shown by the disappearance of the characteristic ^{1}H NMR signals of the hydride and γ-methine moieties as depicted in Scheme 2. Several broad and sharp signals appeared in the formate and in the methine region. To characterize the generated **Mixture 3** of species, a Diffusion-Ordered Spectroscopy (DOSY) NMR experiment (Figure 1, top) was conducted. The self-diffusion dimension reveals two distinct self-diffusion coefficients D of $3.6\cdot10^{-10}$ and $4.2\cdot10^{-10}$ $m^2\cdot s^{-1}$ (Table 1). These coefficients translate to hydrodynamic radii (r_H) of 10.4 and 12.1 Å, attributed to trimeric and tetrameric structures, with respect to the dimeric complex **1** (hydrodynamic radius of 5.9 Å, Table 1). New signals of formate and methine appeared for both trimeric and tetrameric structures, associated with the reactivity with CO_2 (Scheme 2). The formate moieties result from the expected insertion of CO_2 into the Mg–H moiety.

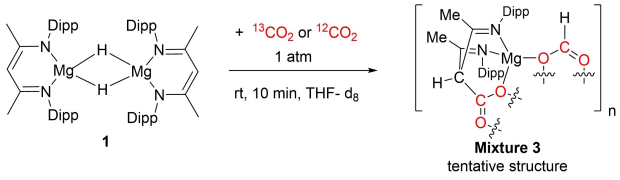

Scheme 2. General scheme for the reactivity of BDI Mg hydride complex **1** with CO_2 at room temperature in THF-d_8 yielding **Mixture 3** with n = 3 and 4.

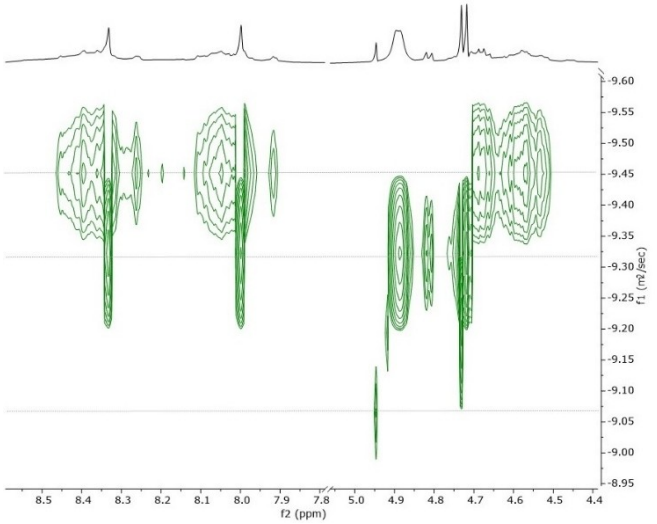

Figure 1. ^{1}H 2D-DOSY NMR spectrum of **Mixture 3-^{13}C** in THF-d_8 at 293 K using the exponential processing method in TopSpin 4.1.4 software. The horizontal scale (F2 axis) shows the ^{1}H chemical shifts (ppm), while the vertical dimension (F1 axis, log m^2/s) shows the diffusion coefficient scale. The self-diffusion coefficients (D) (unit; $\times10^{-10}$ $m^2\,s^{-1}$) given in the spectrum were obtained by regression analysis by fitting the peak intensity and peak areas (in the range of 8.94–7.65 ppm) of the formate signals to the Stejskal-Tanner equation from the T1/T2 module in TopSpin 4.1.4 software. Bottom: ^{1}H NMR spectra of the formate and methine region. Signals that correspond to trimer are assigned to (*), and signals of tetramer are assigned to (#).

Table 1. Diffusion coefficients D (10^{-10} $m^2 s^{-1}$) obtained by DOSY NMR experiments, calculated hydrodynamic radii r_H (Å) in solution and solid state, and nuclearities of the oligonuclear magnesium complexes.

Complex	D[a]	r_H[b] in solution	r_H[c] in solid state	Aggregation degree
1	7.5	5.9	6.8[c]	Dimer
2	6.0	7.3	7.3[c]	Dimer
Mixture 3	3.6, 4.2	12.1, 10.4	–	Tetramer, trimer
4-THF	2.5[d]	17.2	17.3	Hexamer
4-Tol	2.1	17.6	–	Hexamer

[a] The diffusion coefficients were determined by regression analysis by fitting the peak areas to the Stejskal-Tanner equation from T1/T2 analysis module in Topspin 4.1.4 software. The diffusion coefficients are the average values derived from the concentration range of 18–55 mM to reduce the effect of viscosity change and intermolecular interactions. The uncertainty of the diffusion constants obtained from T1/T2 analysis is D ± 0.1. [b] r_H = hydrodynamic radius. The diffusion coefficient and hydrodynamic radii are correlated theoretically by the Stokes-Einstein relation ($D = (kT)/(6\pi\eta r_H)$). [c] The hydrodynamic X-ray radii of complexes **1** and **2** were calculated as reported in the literature by using the published X-ray crystallographic data.[36,37] [d] Supernatant in the reaction solution which generated sparingly soluble **4-THF**.

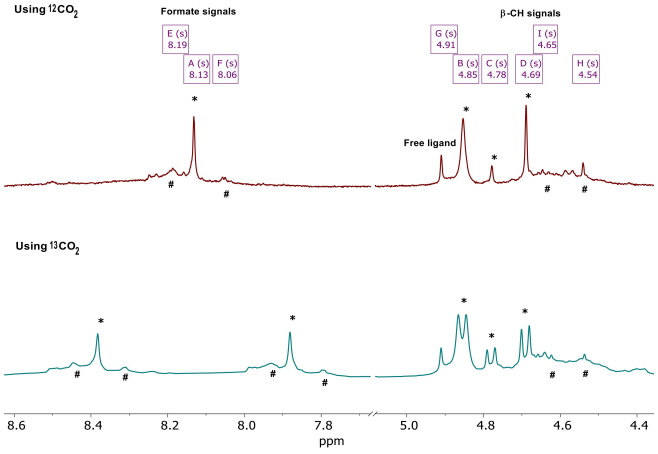

Figure 2. ^{1}H NMR spectra of the formate and methine region of **Mixture 3-^{13}C**. Signals that correspond to the trimer are marked with an asterisk (*) and signals of the tetramer with #.

In the ^{1}H NMR spectrum, a sharp doublet appears at 8.13 ppm ($^1J_{C-H}$ = 200.0 Hz) which correlates with a singlet at 169.4 ppm in $^{13}C\{^1H\}$ NMR experiments (Figures 1 and 2). These signals are attributed to the trimeric structure by DOSY, while broad formate signals at 8.19 ($^1J_{C-H}$ = 206.5 Hz) and 8.06 ($^1J_{C-H}$ = 205.8 Hz) are attributed to tetrameric structures (Figure 1). The new methine signals are attributed to the reaction of the nucleophilic γ-CH with CO_2, forming a C-C bond, as shown by the characteristic chemical shift of the CH methine signals coupling with the carbon of $^{13}CO_2$ (Figures 1 and 2). For the trimeric structure, three doublets are observed at 4.85 ($^2J_{C-H}$ = 8.3 Hz), 4.78 ($^2J_{C-H}$ = 8.1 Hz) and 4.69 ($^2J_{C-H}$ = 8.1 Hz) ppm in the ^{1}H NMR spectrum. These doublets resolve to singlet with $^{12}CO_2$ or when a $^1H\{^{13}C\}$ NMR analysis is conducted (Figure 2). The presence of several γ-CH–CO_2 signals may be due to the presence of different isomers in solution. Piers *et al.* also observed different isomers with Sc dimers by ^{1}H NMR, depending on the orientation of the BDI ligand.[4,38] We assume that in the case of the trimer, the number of possible isomers increases compared to the dimer. Another explanation for the observation of several signals could have been that not all the γ-CH had reacted, which was also observed by Piers *et al.*[4] However, no modification of the ratio of the three γ-CH–$^{13}CO_2$ signals was observed over time and when different pressures (0.5, 1, 3 or 5 atm) of CO_2 were applied (Figure S6), only the relative ratio of free ligand at 4.91 ppm. Moreover, no signal of the ligated β-diketiminate of complex **1** is observed in ^{1}H or ^{13}C NMR spectra. In the HSQC experiment, the ^{1}H signals of the γ-CH correlate with a ^{13}C signal around $\delta_{13C} \approx 70$ ppm, which is significantly different from the characteristic chemical shift of δ_{13C} = 91 ppm for the sp^2 γ-CH of the starting complex **1**. For the tetrameric form, two broad signals appear at 4.65 and 4.54 ppm in the ^{1}H NMR spectrum (Figures 1 and 2). In these signals, there is no clear evidence of coupling with the ^{13}C nucleus, because the signals are too broad. Nonetheless, we assume that they correspond to γ-CH–$^{13}CO_2$ because of the signal of the trimeric forms and because the trimeric and tetrameric species are involved in exchange processes. The EXSY experiments in ^{1}H and in ^{13}C NMR indeed indicate that the β-CH–$^{13}CO_2$ signals of the trimeric species are in exchange with each other and with the signals of the tetrameric forms. The reversibility of the reactivity of CO_2 to afford **Mixture 3** was investigated with a labeling experiment. An NMR tube containing a labeled **Mixture 3-^{13}C** was degassed and pressurized with 1 atm of $^{12}CO_2$ gas at ambient temperature. In those conditions, exchange of the γ-CH–$^{13}CO_2$ signals for the β-CH–$^{12}CO_2$ occurred within 1 h at room temperature, while the peaks of the formate group remained unchanged (Figures S15 and S16). This feature is like what has been observed by Hill *et al.* in the case of **G** that also exchange CO_2 in the γ-CH–$^{13}CO_2$ position, but not at the formate ligands.

Interestingly, when **Mixture 3** is cooled below −40 °C, the formate and γ-CH signals associated with trimeric structures completely disappeared, presumably in favor of the tetrameric structures (Figure S4). This process was reversible. On the contrary, raising the temperature up to 55 °C did not lead to major changes. At this stage, the NMR analysis proved that CO_2 reacted with complex **1** both at the Mg–H and the γ-CH moieties similarly to what was observed by Hill *et al.* with complex **F**. However, in absence of $B(C_6F_5)_3$, it is not a dimeric structure which was generated but a mixture of trimers and tetramers. Beyond the difference to complex **G**, the formation of polynuclear carboxylate species with a BDI ligand is unprecedented to the best of our knowledge. Nevertheless, a hexanuclear complex with (BDI)Mg units had been observed earlier during reductive hexamerization of CO with Mg(I)

compounds yielding the central benzene-1,2,3,4,5,6-hexakis(olato) compound.[39] We propose that the formate moiety generated from the CO_2 insertion into the Mg–H bond of **1** participates in the formation of the polynuclear structure as either a bidentate or a tridentate bridging entity as depicted in Scheme 2. Formate moieties are indeed classical bridging fragments in dimer complexes, such as e.g. in complex **G**.

Generation and characterization of the hexameric complex 4-THF and 4-Tol. When **Mixture 3** was heated at 60 °C for four days, crystals of complex **4-THF**, suitable for the XRD analysis, precipitated in the NMR tube during the heating process. The crystallization process reproducibly yielded complex **4-THF** in high yields ranging between 77 and 81 %. This feature indicated that the trimeric and tetrameric structures of dissolved **Mixture 3** was converted to **4-THF** for a very large extent. The formation of **4-THF** is depicted in Scheme 3.

Molecular structure and atom labelling of **4-THF** are depicted in Figure 3. The resolution of the crystallographic analysis is rather low because of low diffraction power most certainly due to the very large number of atoms per molecule (258 atoms excluding hydrogen) and disordering at the periphery. Complex **4-THF** is a hexameric structure that crystallizes in the cubic space group $Pa\bar{3}$ with a crystallographic center of inversion, making the six Mg sites identical. Each Mg center adopts an octahedral geometry stabilized by six oxygen atoms as depicted in Figure 4. While three oxygen atoms arise from bridging formate ligands (O1, O2′, and O2″) with an av. Mg–O bond length of 2.089 Å, a fourth one belongs to a coordinated THF molecule with a significantly larger Mg1–O5 distance of 2.159(6) Å due to lack of electrostatic attraction. The two remaining oxygen atoms O3 and O4 come from bridging carboxylate moieties (av. Mg–O 2.017 Å) arising from the reactivity of CO_2 with the γ-C atom of the β-diketiminato ligand.

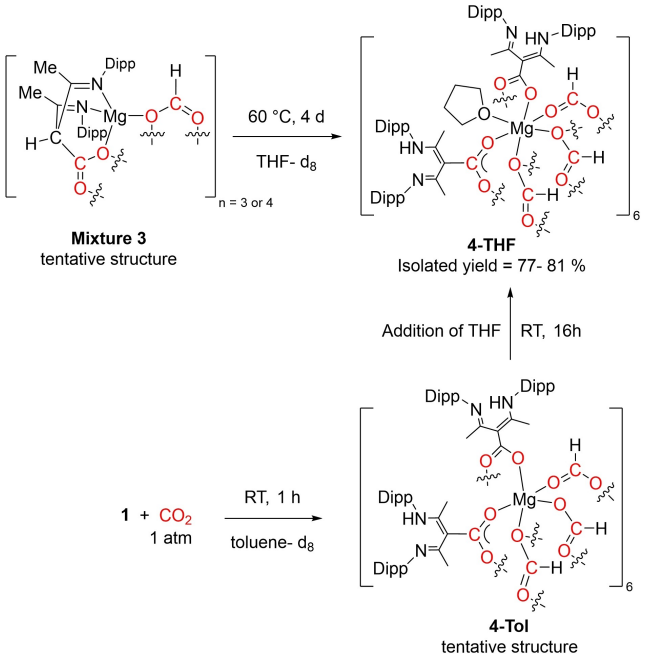

Scheme 3. General scheme for the reactivity of hydride complex **1** with CO_2.

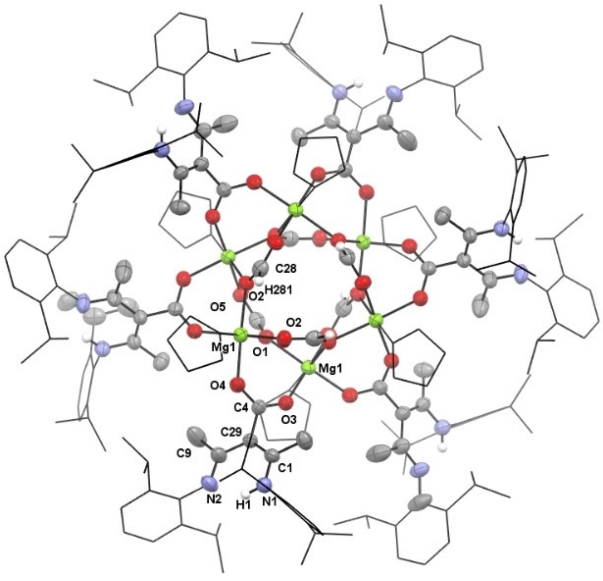

Figure 3. ORTEP representation of the molecular structure of hexanuclear **4-THF** with selected atom labelling. Displacement ellipsoids are set at 30 % probability, C-bound H atoms are omitted for clarity except those of the formate ligands. Visualization for 2,6-iPr$_2$C$_6$H$_3$ (Dipp) and ligated THF has been set as wireframes for clarity.

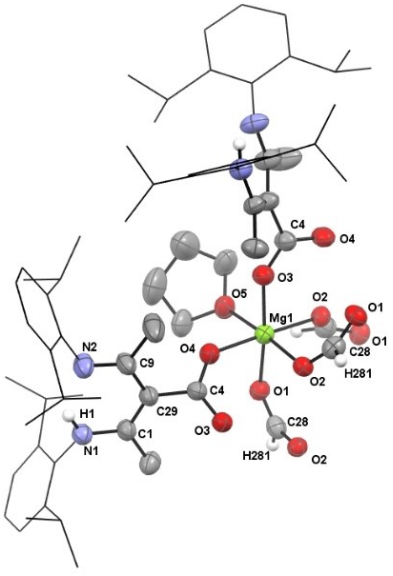

Figure 4. Coordination sphere of Mg1 of **4-THF** with selected atom labelling. Displacement ellipsoids are set at 30 % probability, All H atoms are omitted for clarity except those on N and on the formate ligands. Visualization for 2,6-iPr$_2$C$_6$H$_3$ (Dipp) has been set as wireframe for clarity reasons. Selected bond lengths (Å): Mg1–O1 2.087(5), Mg1–O2′ 2.086(5), Mg1–O2″ 2.095(5), Mg1–O4 2.006(5), Mg1–O5 2.159(6), O2–C28 1.261(8), O1–C28 1.230(8), O4–C4 1.247(8), O3–C4 1.266(8), N1–C2 1.443(8), N1–C1 1.338(8), N2–C9 1.292(9).

The two nitrogen atoms of the ligand are not coordinated anymore and are replaced by the carboxylate moieties that bridge the Mg centers. The γ-CH proton has shifted to one of the nitrogen atoms of the BDI ligand leading to an amino-imine fragment with an N–H···N hydrogen bridge. Overall, the complex structure can be described as a crown of six Mg centers, forming a chair, where the Mg atoms are connected inside the crown by the six formate ligands and outside by the six carboxylate moieties of the originally β-diketiminato ligands, the N(Dipp) and N(H)(Dipp) fragments pointing in the exterior of the crown.

The IR spectrum of solid **4-THF** exhibits characteristic absorbances associated with C=O carbonyl stretching vibrations of the formate moiety at 1617 (s) and 1659 (s) cm^{-1} for $^{13}CO_2$ and $^{12}CO_2$, respectively (Figure S22). This difference of 42 cm^{-1} is comparable to the 45 cm^{-1} difference observed in polycarbonate compounds obtained from the copolymerization of propylene oxide with $^{13}CO_2$ instead of $^{12}CO_2$.[40]

The characterization of complex **4-THF** in solution was challenging because the crystalline compound is insoluble in common organic solvents (THF, toluene, benzene, *n*-pentane, CH_3CN, chloroform, dichloromethane, and DMSO) and could neither be dissolved at room temperature nor during heating at 60 °C for 16 h. Nonetheless, the *in-situ* monitoring of the transformation and crystallization of **4-THF** in the NMR tube showed the disappearance of the signals associated with **Mixture 3** and the appearance of a new broad signal at 8.13 ppm in ^{1}H NMR analysis, attributed to a formate moiety while the γ-CH–$^{13}CO_2$ signals were replaced by a single NH signal at 13.26 ppm in ^{1}H NMR experiments. Moreover, these new signals are associated with a diffusion coefficient of $2.5 \cdot 10^{-10}$ $m^2 \cdot s^{-1}$ in DOSY NMR analysis (Table 1), corresponding to a hydrodynamic radius of 17.2 Å in agreement with the hydrodynamic radius of 17.3 Å derived from the X-ray diffraction analysis of hexameric **4-THF**.

Then the reaction of complex **1** with CO_2 was repeated in toluene instead of THF. As in THF, CO_2 readily reacted at room temperature with the Mg–H and the γ-CH moieties of complex **1** within 1 h. However, these transformations were associated with the concomitant flip of the BDI ligand. While a formate signal is indeed observed at 8.41 (broad signal) and 170.2 ppm in ^{1}H and ^{13}C{^{1}H} NMR analyses, respectively, the only observed γ-CH signal corresponds to free ligand that was released during the process. In ^{1}H NMR, the N(H)(Dipp) signal of free ligand appeared at 12.36 ppm and a new signal attributed to the N(H)(Dipp) moiety of a BDI ligand coordinated by the carboxylate moiety formed during the reaction of CO_2 with the γ-CH moiety. Besides the free ligand, the DOSY experiment indicated a single self-diffusion coefficient of $2.1 \cdot 10^{-10}$ $m^2 \cdot s^{-1}$ (Figure 5), corresponding to a hexameric structure (Table 1). No crystal could be grown in those conditions but based on the crystal structure of **4-THF** and a very similar NMR signature of –NH, –OCHO, –COO groups in ^{1}H and ^{13}C{^{1}H} NMR analyses, we propose the hexameric structure depicted in Scheme 3. This structure is analogous to the structure of **4-THF**, except for the presence of one coordinated molecule of THF per metal center. In accordance with this assumption, the addition of THF to the toluene solution of **4-Tol** at room temperature resulted in the formation of crystals of **4-THF** within 16 h in 77% yield. This observation is in agreement with the expectation that large aggregates are generally more accessible in donor-free solvent media.

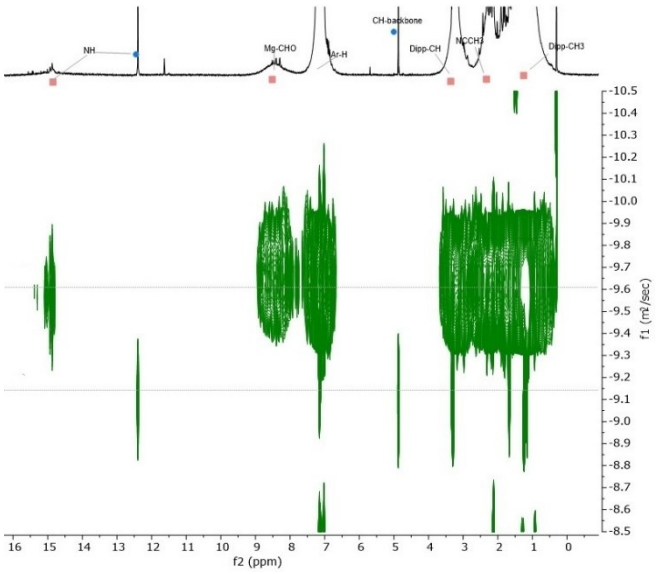

Figure 5. 1H 2D-DOSY NMR spectrum of 4-Tol–^{12}C (red squares) in THF-d_8 at 293 K obtained using the exponential processing method in TopSpin 4.1.4 software. The horizontal scale (F2 axis) shows the ^{1}H NMR chemical shifts (ppm), the vertical dimension (F1 axis, log m^2/s) shows the diffusion coefficient scale. The self-diffusion coefficients (D) (unit; ×10–10 $m^2 s^{-1}$) were obtained by regression analysis by fitting the peak areas of the formate signal (in the chemical shift range of 9.20–7.47 ppm) to the Stejskal-Tanner equation from the T1/T2 module in TopSpin 4.1.4 software.

The reaction of the BDI calcium hydride **2** with CO_2 in THF proceeded much less clearly. In an NMR experiment, the carbon dioxide was consumed within 10 min and the signal of the calcium-bound hydride disappeared at the same time. DOSY NMR measurements revealed that several species with different aggregation degrees were present in solution. However, crystallization efforts generated gel-like materials and we were unable to isolate pure compounds.

Catalytic behavior of 4-THF and 4-Tol in CO_2 hydroboration. We already showed that complex **1** catalyzed the hydroboration of CO_2 into bis(boryl)acetal (BBA) in 79% yield within 7 h 25 min with 9-BBN and in 95% yield within 18 min with $HBCy_2$.[23] We thus probed the use of complex **4-THF** and **4-Tol** under similar catalytic conditions (except that 10 mol% catalyst loading was employed instead of 1 mol%). Application of the insoluble crystals of **4-THF** under heterogeneous reaction conditions led to very minimal hydroboration of CO_2, i.e. less than 4% of BBA formed and comparable to the blank test in absence of catalyst using 9-BBN or $HBCy_2$ as reductants. The soluble complex **4-Tol** similarly resulted in the formation of less than 2% of BBA. Overall, the hexanuclear complexes featuring a flipped BDI ligand were not catalytically active for hydroboration of CO_2. This absence of catalytic properties could result

from insolubility of **4-THF** and/or lack of accessibility of the formate moieties that are embedded in the core of the hexameric structures.

Conclusions

The reaction of CO_2 with Mg and Ca hydride complexes bearing, a bulky β-diketiminato ligand, has been studied in detail. The investigation shows that CO_2 reacts both at the hydride site and at the γ-CH site of the β-diketiminato ligand. These findings are in accordance with the reactivity of CO_2 toward Sc and Mg complexes reported earlier and more generally with the known ability of the β-diketiminato ligand to react via its nucleophilic γ-CH site. This reactivity leads to the decoordination of the imine moieties allowing the coordination via the newly formed carboxylate site associated with a proton shift from the γ-CH to one imine moiety. This ligand flip was less documented, and we show herein that it can occur with the Mg hydride complex under different reaction conditions depending on solvent and temperature. The flipping of the BDI ligand in this work aligns well with the hard soft acid base (HSAB) concept with hard Mg^{2+} favoring bonding to the hard O rather than to the softer N atoms. Moreover, so far only monomeric and dimeric structures have been reported from the reactivity of complexes bearing bulky β-diketiminato ligands, but in this study trimeric, tetrameric, and even hexameric structures are generated. Diffusion-Ordered Spectroscopy (DOSY) NMR experiments are instrumental to understand these intricate mixtures of compounds and to highlight the dynamic exchange occurring between these structures depending on solvent and temperature.

Experimental Section

General. All reactions with air and moisture sensitive compounds were carried out using standard Schlenk line and glovebox techniques under inert atmosphere of either nitrogen or argon. Solvents were dried either over KOH and subsequently distilled over sodium/benzophenone under nitrogen atmosphere or using an MBraun SPS column prior to use. Deuterated solvents were dried either over sodium, degassed, and distilled under nitrogen atmosphere and stored under nitrogen with sodium or freeze-pump-thaw degassed and stored under argon over 4 Å molecular sieves. All substrates were purchased from Alfa Aesar, abcr, SigmaAldrich, or TCI and used without further purification. The purity of the compounds was controlled by NMR spectroscopy. Quick Pressure Valve NMR tubes were used for the reactions with CO_2. NMR experiments were conducted in pressurizable NMR tubes. ^{1}H and $^{13}C\{^{1}H\}$ NMR spectra were recorded on Bruker Avance III 400 (BBO, BBFO probes), Avance II HD 500 (BBO Prodigy probe), and Avance neo 500 (BBFO Prodigy probe) spectrometers. Chemical shifts are relative to $SiMe_4$ for ^{1}H and ^{13}C analyses and for ^{11}B analysis to $F_3B{\cdot}Et_2O$. Chemical shifts are reported in parts per million and coupling constants in Hz. Complexes **1**[8] and **2**[9] were synthesized according to literature procedures.

Reaction of complex 1 with CO_2 in THF at room temperature: generation and characterization of Mixture 3. A pressurizable NMR tube was charged with complex **1** (20 mg, 0.022 mmol) and 0.65 ml of THF-d_8. The solution was degassed, and the sample was exposed to 1 atm of dynamic CO_2 for 3 min before the tube was closed. ^{1}H and $^{13}C\{^{1}H\}$ NMR spectra were collected at 298 K after 10 min. The tetrameric and trimeric nature of the two species was determined by DOSY experiment. The dynamic exchange of the peaks between tetrameric and trimeric forms was observed by EXSY with the signal of the C*H*-backbone of the ligand.

In situ characterization of the trimeric form (n = 3) in Mixture 3-^{13}C: ^{1}H NMR (400 MHz, 298 K, THF-d_8): δ 8.13 (d, $^{1}J_{CH}$ = 200.5 Hz, Mg–OC*H*O), 6.92–7.14 (m, Ar–*H*), 4.69, 4.78, 4.85 (d, $^{2}J_{CH}$ = 8.7 Hz, C*H*-backbone), 2.96, 3.03, 3.12 (sept, Dipp–C*H*$(CH_3)_2$), 1.89, 1.93, 1.95 (s, NCC*H*$_3$), 1.12 (m, Dipp–CH(C*H*$_3$)$_2$), 1.08 (m, Dipp–CH-(C*H*$_3$)$_2$). **$^{13}C\{^{1}H\}$ NMR** (101 MHz, 298 K, THF-d_8): δ 180.1–182.3 (Mg–O*C*O), 170.5 (Mg–O*C*HO), 160.4 (N*C*CH$_3$), 137.4 (Ar–*C*), 124.8 (Ar–*C*), 123.7 (Ar–*C*), 28.6 (CH(CH$_3$)$_2$), 24.6 (CH(*C*H$_3$)$_2$), 24.5 (CH(*C*H$_3$)$_2$), 24.0 (CH(*C*H$_3$)$_2$), 21.1 (NC*C*H$_3$), **^{1}H DOSY NMR** (600 MHz, 298 K, THF-d_8): D = 4.2×10^{-10} m^2 s^{-1}; R_H = 10.4 Å.

In situ characterization of the tetrameric form (n = 4) in Mixture 3-^{13}C: ^{1}H NMR (400 MHz, 298 K, THF-d_8): δ 8.22 (m, Mg–OC*H*O), 6.92–7.06 (m, Ar–*H*), 4.38–4.66 (m, C*H*-backbone), 2.63–3.03 (br, Dipp–C*H*$(CH_3)_2$), 1.80 (br, NCC*H*$_3$), 0.93–1.18 (br, Dipp–CH-(C*H*$_3$)$_2$). **$^{13}C\{^{1}H\}$ NMR** (101 MHz, 298 K, THF-d_8): δ 176.8 (Mg–O*C*O), 169.4–171.9 (Mg–O*C*HO), 137.4 (Ar–*C*), 124.3 (Ar–*C*), 123.7 (Ar–*C*), 28.6 (*C*H(CH$_3$)$_2$, overlapping with THF-d_8), 24.5 (CH(*C*H$_3$)$_2$, 23.4 (CH(*C*H$_3$)$_2$), 21.1 (NC*C*H$_3$), The NC*C*H$_3$ carbon nucleus was not detected. **^{1}H DOSY NMR** (600 MHz, 298 K, THF-d_8): D = 3.6×10^{-10} m^2 s^{-1}; R_H = 12.1 Å.

Reaction of 1 with CO_2 in THF at 60 °C: generation and characterization of complex 4-THF. A pressurizable NMR tube was charged with **1** (20 mg, 0.022 mmol) and THF-d_8. The solution was degassed, and the sample was exposed to 1 atm of dynamic CO_2 pressure for 3 min before the tube was closed. After 4 days at 60 °C, colorless crystals, suitable for X-ray analysis, precipitated. The crystalline material was washed with cold THF (3×0.5 ml) and then dried yielding 21.5 mg (0.036 mmol, 81 %) of **4-THF**. The procedure was repeated several times, constantly giving rise to crystals in 77–81 % yield. Crystals of **4-THF** are insoluble in organic solvents such as THF, toluene, benzene, *n*-pentane, CH_3CN, chloroform, dichloromethane and DMSO (at room temperature as well as after heating at 60 °C for 16 h).

Solid-state characterization of crystal 4-THF. Anal. Calcd. for $C_{210}H_{300}Mg_6N_{12}O_{30}$: calcd.: C 69.70, H 8.36, N 4.65; found: C 68.55, H 8.49, N 4.33. The data found for C does not match with the theoretical C value despite several attempts due to carbonate formation during combustion. **IR (solid, v/cm^{1}) of 4-THF-^{13}C**: 2961 (m), 2927 (w), 2869 (w), 1617 (s, νO_2C), 1585 (m, νO_2C), 1524 (s), 1460 (w), 1436 (w), 1393 (s), 1363 (m), 1332 (s), 1272 (m), 1255 (w), 1237 (m), 1192 (w), 1179 (w), 1161 (w), 1101 (w), 1049 (w), 1030 (w), 1018 (w), 955 (w), 934 (w), 926 (w), 839 (w), 815 (w), 804 (w), 786 (s), 779 (s), 772 (s), 755 (m), 705 (w), 678 (w), 659 (w). **IR (solid, v/cm^{1}) of 4-THF-^{12}C**: 2961 (m), 2927 (w), 2868 (w), 1659 (s, νO_2C), 1633 (m, νO_2C), 1599 (m), 1583 (m), 1560 (m), 1533 (s), 1459 (w), 1431 (s), 1405 (s), 1383 (m), 1356 (s), 1324 (m), 1271 (m), 1256 (m), 1237 (m), 1192 (w), 1179 (w), 1160 (w), 1101 (w), 1049 (w), 1030 (w), 1020 (w), 955 (w), 933 (w), 927 (w), 839 (w), 815 (w), 804 (w), 786 (s), 779 (s), 760 (s), 705 (w), 679 (w), 659 (w). The peaks differences of the carbonyl C=O stretch (νO_2C) between **4-THF-^{13}C** and **4-THF-^{12}C** are 42 and 48 cm^{-1}. The NMR analyses of the supernatant show signals indicative of a hexameric structure with formate signals and possibly –NH signals of a coordinated ligand (see Supporting Information). **^{1}H DOSY NMR** (600 MHz, 298 K, THF-d_8): D = 2.5×10^{-10} m^2 s^{-1}; R_H = 17.2 Å. **Dec**. at 133 °C.

Reaction of complex 1 with CO_2: generation and in-situ characterization of compound 4-Tol. A pressurizable NMR tube was charged with complex **1** (20 mg, 0.022 mmol) and 0.65 ml of toluene-d_8. The sample was degassed and exposed to 1 atm of dynamic CO_2 for 3 min before the tube was closed. After 1 h, ^{1}H NMR and ^{13}C {^{1}H} NMR experiments revealed the presence of compound **4-Tol** along with free ligand. The decomposition of **4-Tol** to free ligand was evidenced in ^{1}H NMR by the disappearance of the broad signals of **4-Tol** after a week at room temperature. Addition of 0.1 ml of THF to the toluene-d_8 solution of **4-Tol** and free ligand obtained after 16 h, colorless crystals of **4-THF** precipitated (characterized by the unit cell parameters). Yield: 20.7 mg (0.034 mmol, 77 %).

In situ characterization of 4-Tol-^{13}C: ^{1}H NMR (400 MHz, 298 K, Tol-d_8): δ 14.82 (brs, 1H, N*H*), 8.41 (brd, $^1J_{CH}$ = 160 Hz, 1H, Mg–OC*H*O), 6.99–7.20 (brs, 6H, Ar–*H*), 3.14 (brs, 4H, Dip–C*H*$(CH_3)_2$), 2.19 (brs, 6H, NCCH_3), 1.13 (brs, 24H, Dip–CH(CH_3)$_2$). **^{13}C{^{1}H} NMR** (101 MHz, 298 K, Tol-d_8): δ 178.9 (Mg–OCO), 170.2 (Mg–OCHO), 142.7 (Ar *o*–CH), 141.3 (Ar C^{IV}), 125.4 (Ar *p*–CH), 123.5 (Ar *m*–CH), 28.6 (*C*H$(CH_3)_2$), 24.6 (CH(*C*H_3)$_2$), 23.6 (CH(*C*H_3)$_2$), 20.7 (NCCH_3, overlapping with toluene-d_8 signal). The NCCH_3 and *C*-backbone carbon nuclei were not detected. **^{1}H DOSY NMR** (600 MHz, 298 K, Toluene-d_8): D = 2.1×10^{-10} m^2 s^{-1}; R_H = 17.6 Å. **HRMS (ESI-positive ion) m/z:**. 1478.9363 (3 L + 2Mg + 4OCO) **calcd**. 1478.9333.

Crystal structure determination. Data was collected at low temperature (100 K) on a Bruker Kappa Apex II diffractometer using a Mo–Kα radiation (λ = 0.71073 Å) micro-source, equipped with an Oxford Cryosystems Cooler Device. The structure has been solved using the new dual-space algorithm program SHELXT,[41] and refined by means of least-squares procedures using the program CRYSTALS.[42] The Atomic Scattering Factors were taken from International Tables for X-Ray Crystallography.[43] Hydrogen atoms were placed geometrically and refined using a riding model. All non-hydrogen atoms were anisotropically refined. Although having analyzed large single crystals, on two different types of X-ray sources (Mo and Cu micro-sources), we could measure only low-resolution diffraction patterns. The presented structure is the best result obtained. This low diffraction power is most certainly due to the very large number of atoms per molecule (258 atoms excluding hydrogen), and strong disorders at the periphery. The data collected has a very low resolution (mostly around 1.2 Å, and few very weak reflections around 1.05 Å). There is a poor data/parameter ratio (7 data per parameter instead of 10 expected for a good structure). However, it should be noted that the observed reciprocal space is clean and that the use of ROTAX and TWINROTMAT tools did not result in the detection of a twin.

Supporting Information

Experimental details of the synthesis, NMR and IR spectra of all new compounds, crystallographic and refinement data, kinetic studies on catalytic hydroboration of CO_2. The CIF file of the X-ray structure determination has been deposited at CCDC.[44]

Acknowledgements

This research has received funding from the European Union's Horizon 2020 research and innovation programme under the Marie Skłodowska-Curie grant agreement No. 860322. We acknowledge the valuable support of the NMR service platform at LCC. Open Access funding enabled and organized by Projekt DEAL.

Conflict of Interest

The authors declare no conflict of interest.

Data Availability Statement

The data that support the findings of this study are available in the supplementary material of this article.

Keywords: cage compounds · CO_2 activation · diketiminato magnesium compounds · formate complexes · magnesium

[1] C. Chen, S. M. Bellows, P. L. Holland, *Dalton Trans.* **2015**, *44*, 16654–16670.
[2] C. Camp, J. Arnold, *Dalton Trans.* **2016**, *45*, 14462–14498.
[3] C. E. Radzewich, M. P. Coles, R. F. Jordan, *J. Am. Chem. Soc.* **1998**, *120*, 9384–9385.
[4] F. A. LeBlanc, A. Berkefeld, W. E. Piers, M. Parvez, *Organometallics* **2012**, *31*, 810–818.
[5] N. J. Hartmann, G. Wu, T. W. Hayton, *Dalton Trans.* **2016**, *45*, 14508–14510.
[6] L. A. M. Harris, E. C. Y. Tam, M. P. Coles, J. R. Fulton, *Dalton Trans.* **2014**, *43*, 13803–13814.
[7] M. D. Anker, M. Arrowsmith, P. Bellham, M. S. Hill, G. Kociok-Kohn, D. J. Liptrot, M. F. Mahon, C. Weetman, *Chem. Sci.* **2014**, *5*, 2826–2830.
[8] R. M. Gauld, J. R. Lynch, A. R. Kennedy, J. Barker, J. Reid, R. E. Mulvey, *Inorg. Chem.* **2021**, *60*, 6057–6064.
[9] R. M. Gauld, R. McLellan, A. R. Kennedy, J. Barker, J. Reid, R. E. Mulvey, *Chem. Eur. J.* **2019**, *25*, 14728–14734.
[10] J. R. Lynch, A. R. Kennedy, J. Barker, R. E. Mulvey, *Chem. Eur. J.* **2024**, *30*, e202303373.
[11] S. P. Green, C. Jones, A. Stasch, *Angew. Chem. Int. Ed.* **2008**, *47*, 9079–9083.
[12] S. Harder, J. Brettar, *Angew. Chem. Int. Ed.* **2006**, *45*, 3474–3478.
[13] M. M. D. Roy, A. A. Omaña, A. S. S. Wilson, M. S. Hill, S. Aldridge, E. Rivard, *Chem. Rev.* **2021**, *121*, 12784–12965.
[14] D. Mukherjee, D. Schuhknecht, J. Okuda, *Angew. Chem. Int. Ed.* **2018**, *57*, 9590–9602.
[15] D. Mukherjee, J. Okuda, *Angew. Chem. Int. Ed.* **2018**, *57*, 1458–1473.
[16] S. Brand, A. Causero, H. Elsen, J. Pahl, J. Langer, S. Harder, *Eur. J. Inorg. Chem.* **2020**, *2020*, 1728–1735.
[17] A. Causero, G. Ballmann, J. Pahl, H. Zijlstra, C. Färber, S. Harder, *Organometallics* **2016**, *35*, 3350–3360.
[18] M. Rauch, Z. Strater, G. Parkin, *J. Am. Chem. Soc.* **2019**, *141*, 17754–17762.
[19] M. Rauch, G. Parkin, *J. Am. Chem. Soc.* **2017**, *139*, 18162–18165.
[20] X. Cao, W. Wang, K. Lu, W. Yao, F. Xue, M. Ma, *Dalton Trans.* **2020**, *49*, 2776–2780.
[21] M. Szewczyk, M. Magre, V. Zubar, M. Rueping, *ACS Catal.* **2019**, *9*, 11634–11639.
[22] D. Mukherjee, S. Shirase, T. P. Spaniol, K. Mashima, J. Okuda, *Chem. Commun.* **2016**, *52*, 13155–13158.
[23] W. Huadsai, M. Westerhausen, S. Bontemps, *Organometallics* **2023**, *42*, 2921–2926.

[24] D. Zhang, C. Jarava-Barrera, S. Bontemps, *ACS Catal.* **2021**, *11*, 4568–4575.
[25] S. Desmons, K. Grayson-Steel, N. Nuñez-Dallos, L. Vendier, J. Hurtado, P. Clapés, R. Fauré, C. Dumon, S. Bontemps, *J. Am. Chem. Soc.* **2021**, *143*, 16274–16283.
[26] A. Béthegnies, Y. Escudié, N. Nuñez-Dallos, L. Vendier, J. Hurtado, I. del Rosal, L. Maron, S. Bontemps, *ChemCatChem* **2019**, *11*, 760–765.
[27] S. Bontemps, *Coord. Chem. Rev.* **2016**, *308*(2), 117–130.
[28] S. Desmons, Y. Zhou, D. Zhang, C. Jarava-Barrera, A. Coffinet, A. Simonneau, L. Vendier, G. Luo, S. Bontemps, *Eur. J. Org. Chem.* **2023**, *26*, e202300525.
[29] G. Jin, C. G. Werncke, Y. Escudié, S. Sabo-Etienne, S. Bontemps, *J. Am. Chem. Soc.* **2015**, *137*, 9563–9566.
[30] M. Westerhausen, A. Koch, H. Görls, S. Krieck, *Chem. Eur. J.* **2017**, *23*, 1456–1483.
[31] S. Krieck, A. Koch, K. Hinze, C. Müller, J. Langer, H. Görls, M. Westerhausen, *Eur. J. Inorg. Chem.* **2016**, *2016*, 2332–2348.
[32] M. Westerhausen, J. Langer, S. Krieck, C. Glock, *Rev. Inorg. Chem.* **2011**, *31*, 143–184.
[33] M. Westerhausen, *Coord. Chem. Rev.* **2008**, *252*, 1516–1531.
[34] M. Westerhausen, *Dalton Trans.* **2006**, 4755–4768.
[35] S. Schnitzler, T. P. Spaniol, L. Maron, J. Okuda, *Chem. Eur. J.* **2015**, *21*, 11330–11334.
[36] A. Macchioni, G. Ciancaleoni, C. Zuccaccia, D. Zuccaccia, *Chem. Soc. Rev.* **2008**, *37*, 479–489.
[37] A. W. Black, W. Zhang, G. Reid, P. N. Bartlett, *Electrochim. Acta* **2022**, *425*, 140720.
[38] L. K. Knight, W. E. Piers, R. McDonald, *Chem. Eur. J.* **2000**, *6*, 4322–4326.
[39] A. Paparo, K. Yuvaraj, A. J. R. Matthews, I. Douair, L. Maron, C. Jones, *Angew. Chem. Int. Ed.* **2021**, *60*, 630–634.
[40] G. A. Bhat, M. Y. Darensbourg, D. J. Darensbourg, *Polym. J.* **2021**, *53*, 215–218.
[41] G. Sheldrick, *Acta Crystallogr. Sect. A* **2015**, *71*, 3–8.
[42] P. W. Betteridge, J. R. Carruthers, R. I. Cooper, K. Prout, D. J. Watkin, *J. Appl. Crystallogr.* **2003**, *36*, 1487.
[43] W. Schmitz: *International Tables for X-ray Crystallography* (Ed.: International Union of Crystallography), Vol. IV (Ergänzungsband). The Kynoch Press, Birmingham, England, **1974**, 366 pages incl. tables and subject index; *Kristall und Technik* **1975**, *10*, K120–K120.
[44] Deposition number CCDC-2339792 (for **4-THF**) contains the supplementary crystallographic data for this paper. These data are provided free of charge by the joint Cambridge Crystallographic Data Centre and Fachinformationszentrum Karlsruhe Access Structures service.

Manuscript received: May 13, 2024
Revised manuscript received: June 19, 2024
Accepted manuscript online: June 24, 2024

